SAND2014-4372C

Complex Geometry Effects on Supersonic Cavity Flows

Katya M. Casper*, Justin L. Wagner†, Steven J. Beresh‡, John F. Henfling§,
Russell W. Spillers,¶ and Brian O. M. Pruett‖
Sandia National Laboratories, Albuquerque, NM 87185

The flow over aircraft bays exhibits many characteristics of cavity flows, namely resonant pressures that can create high structural loading. Most studies have represented these bays as rectangular cavities; however, this simplification neglects many features of the actual flight geometry which could affect the unsteady pressure field and resulting loading in the bay. To address this shortcoming, a complex cavity geometry was developed to incorporate more realistic aircraft-bay features including shaped inlets and internal cavity variations. A parametric study of these features at Mach 1.5, 2.0, and 2.5 was conducted to identify key differences from simple rectangular cavity flows. The frequency of the basic rectangular cavity modes could be predicted by theory; however, most complex geometries non-uniformly shifted these frequencies. Geometric changes that constricted the flow such as a leading edge overhang or a sidewall insert tended to enhance cavity modes and create higher pressure fluctuations. Other features, such as a leading edge ramp, lifted the shear layer higher with respect to the aft cavity wall and led to cavity tone suppression. Complex inlet shapes introduced spanwise non-uniformity into the shear layer which also led to a reduction of cavity tones, especially at the aft end of the cavities.

Nomenclature

D	cavity depth (mm)	Re	freestream unit Reynolds number (1/m)
f	frequency (kHz)	St	Strouhal number, fL/U_∞
L	cavity length (mm)	U_∞	freestream velocity (m/s)
M	freestream Mach number	W	cavity width (mm)
P_0	total pressure (kPa)		
q_∞	freestream dynamic pressure (kPa)		

I. Introduction

The flow over aircraft bays can generate significant structural loading caused by resonant pressure fluctuations created in the bay. This resonance is typical of cavity flows, which have been extensively studied over the years.[1,2] The flow over a cavity can set up a feedback loop between the free shear layer and the cavity's acoustic field that creates resonant tones or 'Rossiter' modes in the cavity.[3] This typically occurs in 'open' supersonic cavity flows when the cavity length-to-depth ratio L/D is less than 10.[4] The amplitude of the modes can be quite large, and sound pressure levels (SPL) greater than 170 dB have been reported.[5] The frequencies of these modes in compressible flow can be estimated using Heller and Bliss's semi-empirical

*Senior Member of the Technical Staff, Engineering Sciences Center, Member AIAA, kmcaspe@sandia.gov, (505) 844-1574
†Senior Member of the Technical Staff, Engineering Sciences Center, Member AIAA
‡Distinguished Member of the Technical Staff, Engineering Sciences Center, Associate Fellow AIAA
§Distinguished Technologist, Member AIAA
¶Principal Technologist
‖Senior Technologist

Sandia National Laboratories is a multi-program laboratory managed and operated by Sandia Corporation, a wholly owned subsidiary of Lockheed Martin Corporation, for the U.S. Department of Energy's National Nuclear Security Administration under contract DE-AC04-94AL85000.

method.[6] However, the distribution of the mode amplitudes and their frequencies varies greatly depending on flow condition and cavity geometry.

Previous experiments in rectangular cavities of various width and depth have been conducted to study the unsteady fluctuations and their coupling to store vibration.[7,8] Velocimetry measurements of a rectangular cavity in supersonic flow have shown that the cavity width alters the flow field structure.[9] However, there are limitations when applying this work to actual aircraft bays, which have many complex features that are not captured by a simple rectangular cavity geometry.[10] For example, the incoming flow is not necessarily uniform. The presence of the fuselage on the aircraft is an important difference between flight and almost every wind-tunnel test on a rectangular cavity. Also, the cavity is not necessarily aligned with the incoming flow. Previous studies have shown that both cavities in yaw[11–13] or swept cavities[14] can exhibit different mode amplitude distributions or even mode frequencies in some cases.

Also, at the upstream lip of some aircraft bays, there is a sawtooth pattern or sometimes simply a scoop or embankment that sets up a differential flow expansion. This generates strong streamwise vorticity that entrains high-speed fluid into the bay and can also affect the shear layer structure.[10] The upstream lip of the bay can also be higher above the cavity floor than the downstream edge which changes where the shear layer impinges on the back wall of the cavity. This impingement plays a role in the feedback loop governing the cavity dynamics.[3,15–18] Also, the doors of the aircraft bay alter the cavity dynamics.[10,19–21] For example, open doors can modify the side spillage into the bay or closed doors can act like a lid and affect the cavity resonance. Finally, the internal geometry plays a role in the unsteady dynamics because the width or depth of the cavity varies within the bay. For example, several studies have shown that the presence of a store in the cavity, which alters the cavity volume, can change the cavity resonance.[5,7,8,19,22,23] All of these geometric features may change the acoustic environment within the cavity and thus the vibrational excitation of stores contained within.

Limited work has been done to explore these configurational differences[10,14,16,19,24] and much of this work has focused on the control of pressure fluctuations in these complex geometries, not on understanding the differences from simple geometries. To address this shortcoming, a complex cavity geometry has been designed and fabricated for wind tunnel testing that allows features representing a realistic aircraft-bay geometry to be incorporated one by one. A parametric study of these geometric features was conducted at Mach 1.5, 2.0, and 2.5 to isolate important parameters for the pressure loading in aircraft bays and to investigate the limits of rectangular cavities in representing flight geometry.

II. Experimental Setup

II.A. Sandia Trisonic Wind Tunnel

Experiments are performed in Sandia's Trisonic Wind Tunnel (TWT). This is a blowdown-to-atmosphere facility using air as the test gas. The test section is enclosed in a pressurized plenum. In the supersonic configuration, the top and bottom walls of the nozzle are exchanged to obtain Mach numbers of 1.5, 2.0, 2.5, and 3.0. The full test section is 305 mm high and 305 mm wide; however, in the supersonic configuration, a half-nozzle test section is also available. The lower wall of the planar nozzle is replaced by a wall that extends the inlet contour of the tunnel and then fairs into a flat surface along the centerline of the full test-section. The resulting test section is 152 mm high and 305 mm wide. This provides a flat plate working surface with convenient optical access within the test rhombus in which the supersonic expansion is complete. This also allows the cavity to be integrated into the half-nozzle configuration; the wall curvature for the full nozzle extends nearly to the end of test section. Fig. 1 shows the complex geometry installed on the bottom wall of the half-nozzle configuration.

Typical run conditions for these tests are given in Table 1. The Mach number for the supersonic tests is computed from a centerline static pressure measurement 21.9 cm upstream of the cavity leading edge. The stagnation temperature is held constant at $321 \pm 2K$. The walls of the full test section remain near room temperature at $307 \pm 3K$ and likely are the same for the half-nozzle configuration. Due to tunnel starting constraints, these tests were conducted near the maximum Reynolds number available at each Mach number. Tests were not conducted at Mach 3.0 due to starting concerns.

Table 1. Typical Run Conditions

M_∞	q_∞ (kPa)	P_0 (kPa)	$Re \times 10^6/m$
1.5	113	262	34
2.0	134	371	40
2.5	156	585	51

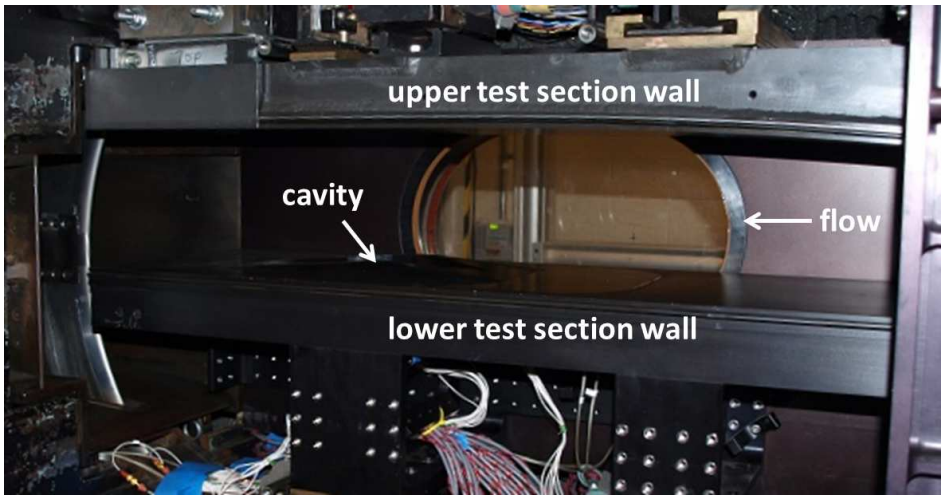

Figure 1. Complex cavity installed in the TWT supersonic half nozzle.

II.B. Cavity design and apparatus

The complex cavity apparatus is built up from a simple rectangular cutout that is integrated into a tunnel wall insert (Fig. 2). This cavity has a length, width, and depth of 203, 102, and 29 mm, respectively. The L/D ratio of 7 categorizes this simple cavity flow as 'open' in supersonic flows.[4] To create distinct complex geometric configurations, different pieces can be added to the front and sides of the rectangular cavity. The basic sensor layout and coordinate system remains the same in the complex geometry. Table 2 lists the various configurations that can be created.

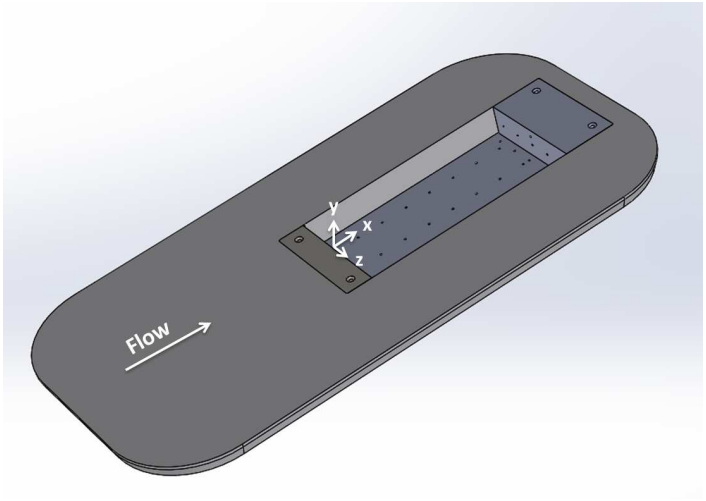

Figure 2. Simple rectangular cavity tunnel insert.

The non-uniform inlet flow found in flight is simulated in the complex geometry with different ramps at the leading edge of the cavity. A smooth 5.7° ramp is the baseline case for comparison (Fig. 3(a)). Two side ramps are also added to this configuration to transition from the higher leading edge to the flat plate

geometry on the sides of the cavity. The front ramp lifts the leading edge of the cavity 12.7 mm above the trailing edge and effectively changes the L/D of the cavity along its length from 5 at the leading edge to 7 at the trailing edge. Although these ramps have planar surfaces rather than curved surfaces like a real aircraft, the difference is expected to have little effect on the results.

The next inlet configuration has a ramp with a centered cutout or scoop (Fig. 3(b)). The scoop addresses the effect the engine inlet has on the incoming flow to the cavity. Some of the flow bypasses the inlets and passes through a narrow channel leading up to the bay. This nonuniform flow then passes over a jagged leading edge with a sawtooth pattern that overhangs the front portion of the bay. A similar tooth can be added to the complex geometry to simulate this configuration (Fig. 3(c)). Additional complex geometry configurations were made with offset cutout and sawtooth designs that exaggerate the asymmetries in the flow and move the resulting vortex away from the centerline of the cavity (Figs. 3(d) and 3(e)).

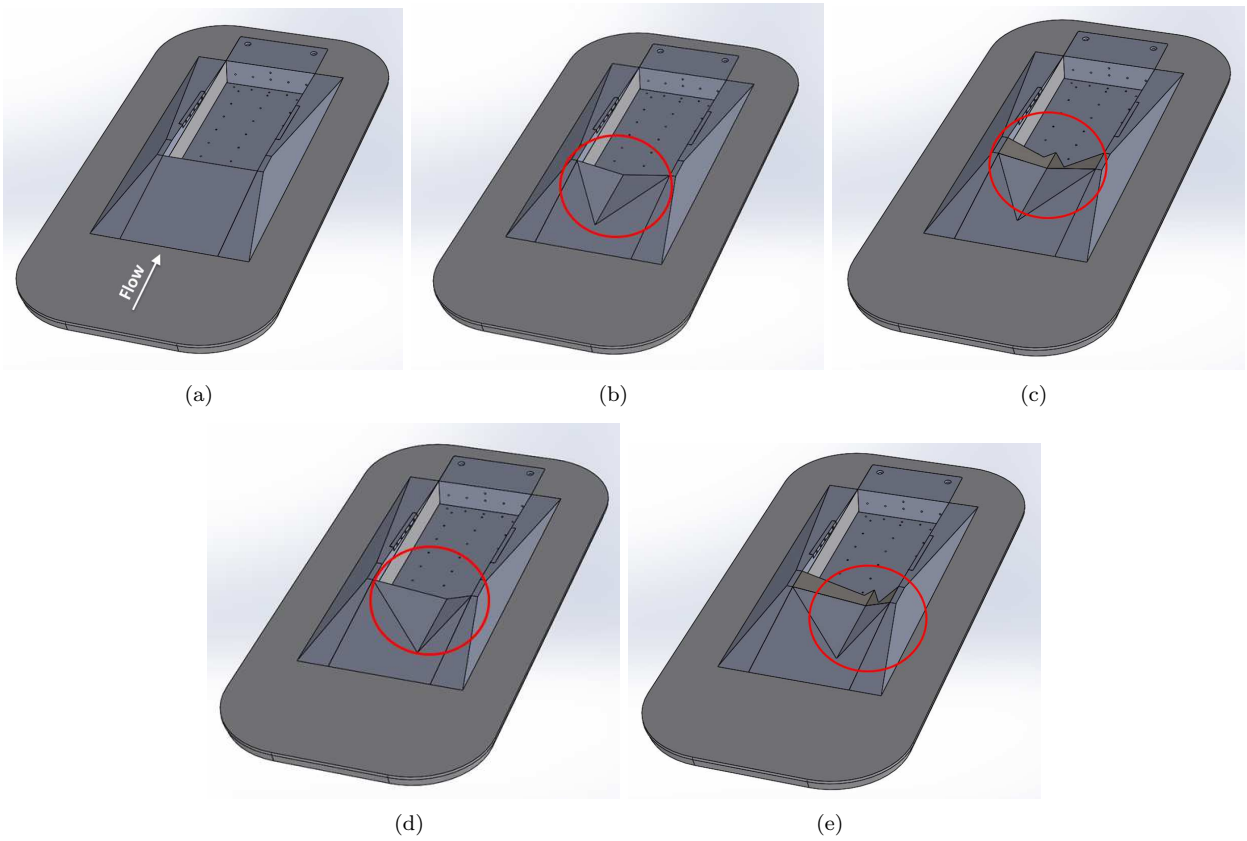

Figure 3. Complex geometry leading edge configurations (a) Smooth ramp; (b) Center scoop (c) Center scoop and tooth; (d) Offset scoop; (e) Offset scoop and tooth.

The internal geometry of the cavity can also be varied. In the actual flight hardware, there is a section at the rear of the aircraft bay containing ductwork. This section effectively decreases the width of the cavity, which will influence the cavity dynamics. An internal insert was designed to simulate this effect (Fig. 4). This insert is 101.6 mm long and 25.4 mm wide, which changes the L/W from 2 to 2.5 over the downstream half of the cavity. Another important parameter is the presence of the aircraft-bay doors, which will affect the cavity dynamics. Unfortunately, the doors could not be incorporated into the supersonic testing because of the additional blockage created by the doors.

II.C. Instrumentation and Data Acquisition

The complex geometry has forty positions available for pressure measurements, thirty of which were used during testing. Five sensors are located in the spanwise direction along the forward floor of the cavity (FFP1–5, Fig. 5(a)). There is also a line of sensors down the center of the cavity (C2-C7). Two sensors are located on either side of sensor C4 in the spanwise direction and are designated L4 and R4. There is another spanwise line of sensors at the rear of the cavity (RFP1–5), as well as at the aft wall of the cavity

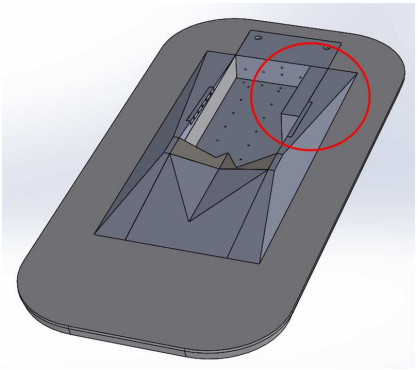

Figure 4. Complex geometry side insert. This changes the width of cavity along its length.

Table 2. Complex geometry configurations.

Configuration	Side Ramps	Front Ramp	Tooth	Side Insert
Simple rectangular cavity	No	No	No	No
Baseline cavity	Yes	Smooth	No	No
Baseline cavity with side insert	Yes	Smooth	No	Yes
Baseline cavity with center scoop	Yes	Center scoop	No	No
Baseline cavity with center scoop and tooth	Yes	Center scoop	Center	No
Baseline cavity with center scoop and tooth and side insert	Yes	Center scoop	Center	Yes
Baseline cavity with offset scoop	Yes	Offset scoop	No	No
Baseline cavity with offset scoop and tooth	Yes	Offset scoop	Offset	No
Baseline cavity with offset scoop and tooth and side insert	Yes	Offset scoop	Offset	Yes

(AWP1–5, Fig. 5(b)). A final sensor AWP6 is located on the cavity centerline, on the aft wall above sensor AWP3. A schematic of these locations with respect to the cavity geometry is shown in Fig. 5(c). When the centered tooth is installed, the front floor sensors FFP1-5 are located beneath an overhang created by the tooth. Sensor C2 is just downstream of the tooth on the cavity floor. When the side insert is installed, sensor R4 is located in front of the insert, while sensors RFP5 and AFP5 are covered.

Kulite XCQ-062-30A (or similar) pressure transducers are used to measure the unsteady cavity pressure fluctuations. These sensors have a resonant frequency of 240–300 kHz. The repeatability is approximately 0.1% of the full scale. The Kulite signal output is passed through an Endevco Model 136 DC Amplifier. This provides a 10 V excitation and is also used to supply a gain of 50–100. A Krohn-Hite Model 3384 Tunable Active Filter is used to provide a 50 kHz anti-aliasing low-pass Bessel filter. This filter has eight poles and provides 48 dB attenuation per octave. The Kulite sampling frequency is typically 500 kHz. Data are acquired using a National Instruments PXI-1042 chassis with 14-bit PXI-6133 modules (10 MHz bandwidth).

III. Experimental Results

III.A. Simple rectangular cavity measurements

Simple rectangular cavity measurements were made to compare to typical results in the literature. Fig. 6 shows the power spectral density of pressure fluctuations in the cavity at Mach 1.5. The power spectra are shown in sound pressure level (SPL) and were computed using Welch's periodogram method, Blackman windows, and 50% overlap between data segments. The frequency resolution of the spectra is 10 Hz.

Resonant peaks corresponding to the Rossiter modes can be clearly seen. The frequencies of these peaks can be compared with the empirical correlation of Heller and Bliss.[6] Fig. 6(a) shows the first ten predicted mode frequencies marked with dashed lines. Similar to Ref. 25, empirical constants of $\alpha = 0.25$ and $K = 0.66$ were used and gave reasonable agreement with the data. The flow in the rectangular cavity shows good symmetry about the centerline. There are small spanwise differences in the spectra, mostly in the level of broadband frequency content which is lowest on the centerline. However the frequency of modes remains constant across the span (Fig. 6(d)). The broadband fluctuations and modal peaks generally increase in amplitude with downstream distance (Fig. 6(b)). However, some modes seem to have nodes along the cavity floor and are not picked up at some locations. For example, mode 2 does not show up in sensor

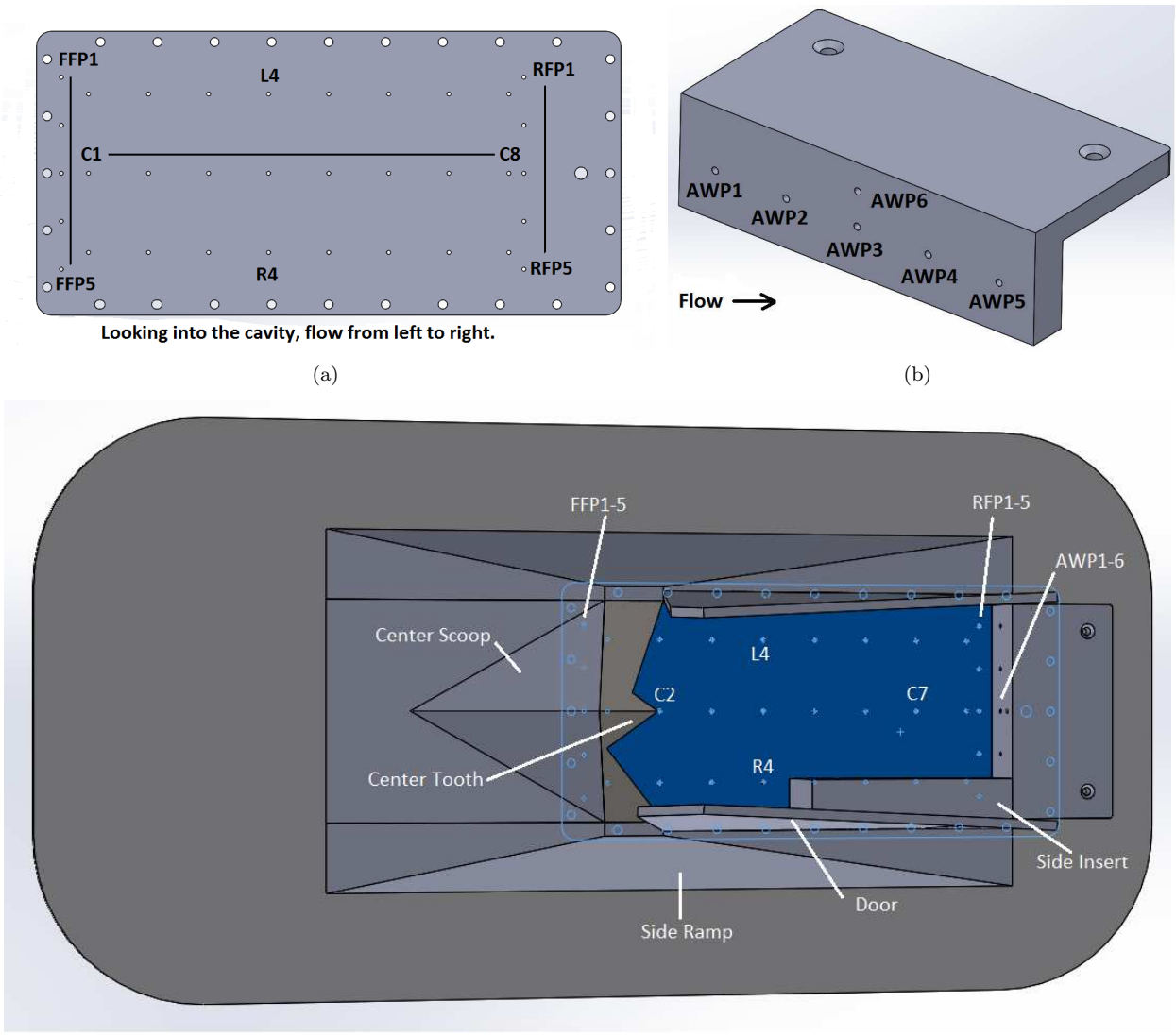

Figure 5. Complex cavity sensor locations (a) Floor plate; (b) Aft cavity wall; (c) Floor plate and aft cavity wall installed in complex geometry.

C6 while mode 3 is absent in sensor C7.

Fig. 7 shows the simple rectangular cavity results along the cavity centerline at all three supersonic Mach numbers. The spectra are normalized by the freestream dynamic pressure to collapse cavity fluctuations at different Reynolds numbers.[26,27] As the Mach number increases, the amplitude of the Rossiter modes decreases with respect to the broadband fluctuations, consistent with observations by Refs. 5 and 6. Sensor node locations also vary with Mach number. However, the second mode still remains dominant, and the frequency of the modes still maintains good agreement with the predicted Rossiter frequencies.

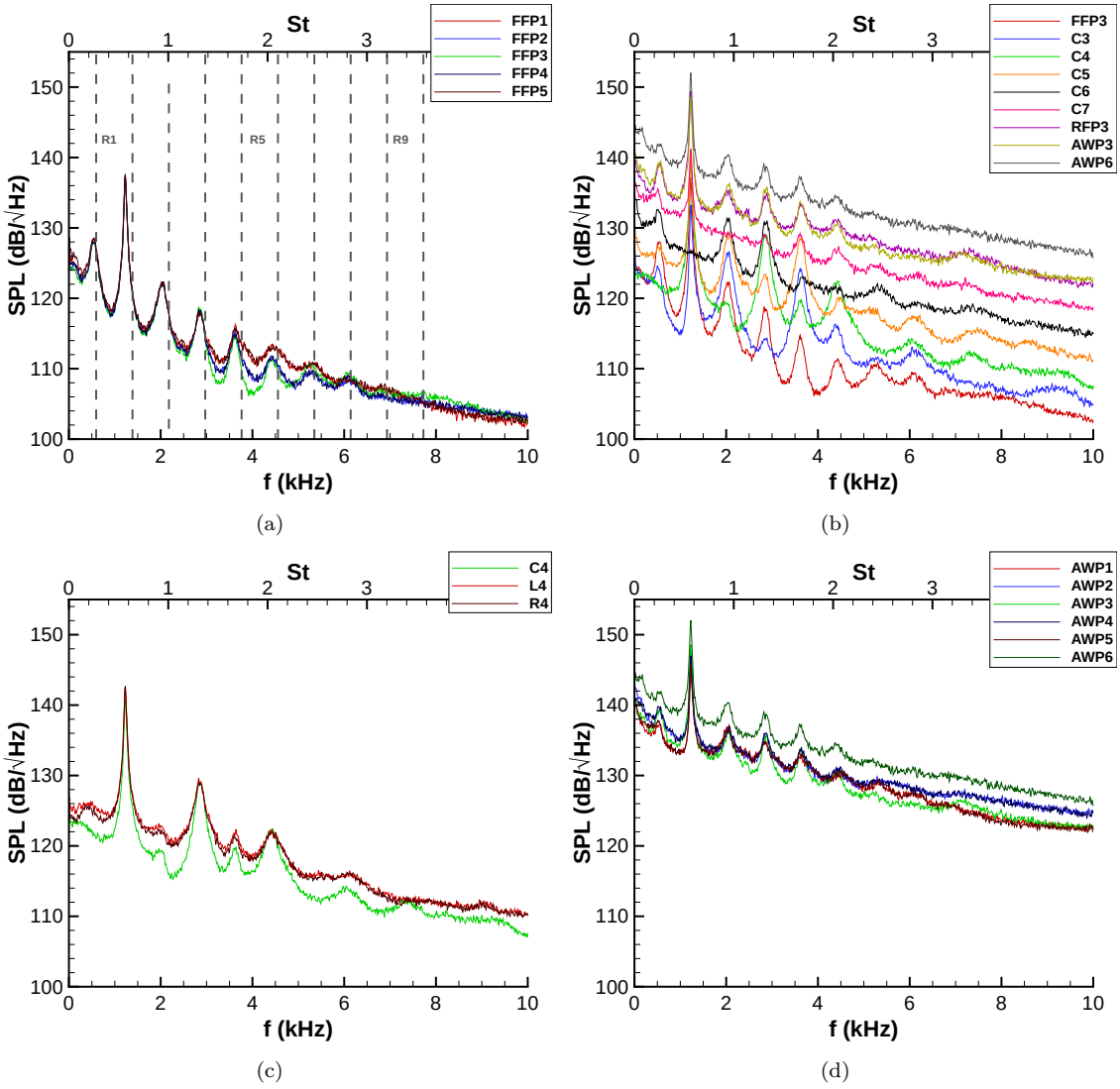

Figure 6. Power spectral density of pressure fluctuations in the simple rectangular cavity at Mach 1.5 (a) Front floor sensors; (b) Centerline sensors; (c) Spanwise sensors, cavity midline; (d) Aft wall sensors.

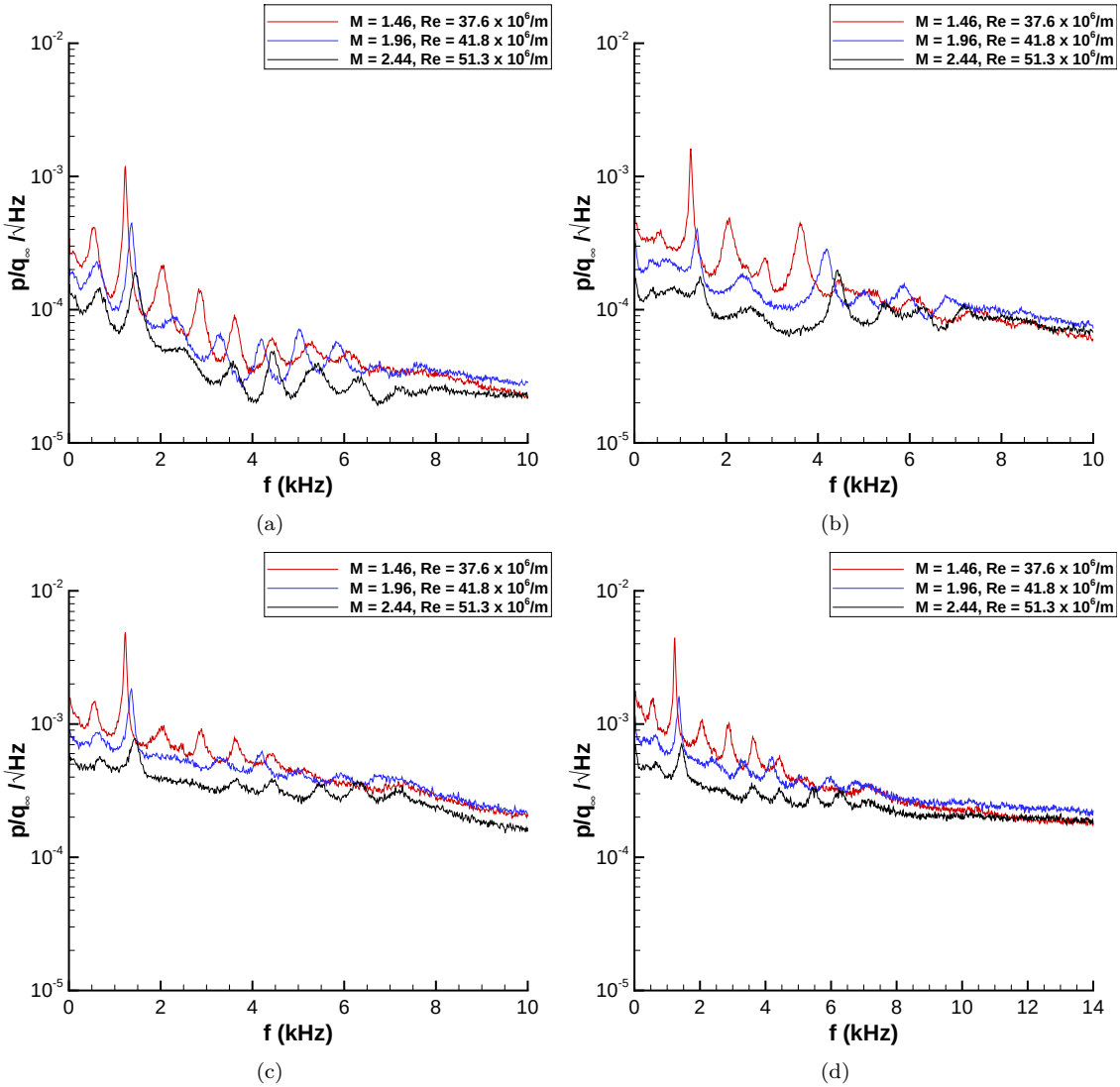

Figure 7. Power spectral density of pressure fluctuations in the simple rectangular cavity at varying Mach number (a) FFP3; (b) C5; (c) RFP3; (d) AWP6.

III.B. Baseline cavity measurements

Similar measurements were made with the baseline cavity configuration. As shown in Fig. 3(a), smooth front and side ramps are added to the rectangular cavity to reach this configuration. Fig. 8 shows a comparison of the PSD's from the centerline of the two geometries. There are significant differences between the two configurations in both the mode amplitude and frequencies. In the baseline cavity, the frequency of the first two modes shifts slightly by about 50 Hz. However, the frequency of the higher modes shifts up much more, between 100–300 Hz. This upward shift would be expected for a deeper cavity; however, Heller and Bliss predictions for L/D ratios of 6 and 7 predict a much larger shift than what is observed in the experiment. There are also large amplitude variations when comparing the simple and baseline cavities. For the baseline cavity, the second mode has a much lower amplitude and modes five through seven have a much higher amplitude when compared to the rectangular cavity. Also, the baseline cavity has higher broadband fluctuations at the front of the cavity, but much lower broadband fluctuations at the rear.

The large difference in both broadband fluctuations and mode amplitudes at the aft wall likely comes from the raised leading edge of the baseline configuration which lifts the shear layer higher with respect to the rear cavity wall. Previous flow control studies have shown that mode amplitudes can be reduced by this lofting, for example by using a leading edge spoiler, which changes the feedback loop that typically creates the resonant pressure fluctuations in the cavity.[3,15–18]

To further look at the nature of the cavity flow, the cross correlation between pressure measurements at the front and rear of the cavity was computed (Fig. 9). A marked difference can be seen between the two geometries. The simple rectangular cavity has much higher correlation levels. The cross correlation is also strongly periodic in nature, showing the coherent and ordered structure of the flow in the rectangular cavity. The time lag corresponding to this dominant periodicity corresponds to 1.28 kHz, the frequency of the dominant second mode observed in the PSD's for the simple rectangular cavity.

On the other hand, the baseline cavity cross correlation shows very little periodicity. There is one large peak near 1 ms corresponding to the time it takes for acoustic disturbances in the cavity to propagate between the two sensor locations. This propagation time is similar to that computed using the phase speed constant in the Heller and Bliss correlation, though slightly lower. This lower propagation time corresponds to higher mode frequencies, consistent with the shift seen in the PSD's when compared to the rectangular cavity. Otherwise, there is no dominant periodicity in the cross correlation as was seen in the simple rectangular cavity. Higher frequency modes in the baseline cavity are more important to the overall pressure fluctuations, but are less correlated than in the rectangular cavity. This result is consistent with the strong second-mode peak for the rectangular cavity PSD but weak amplitudes for all modes in the baseline case.

A comparison of the coherence between fore and aft wall pressure measurements in both configurations can also be made (Fig. 10). At the front of the rectangular cavity, the coherence is near a value of one for the first three modes and then drops for the higher modes. For the baseline cavity, the coherence at the fore wall is lower than the rectangular cavity for the first five modes; however, higher frequency modes show greater coherence levels up to a maximum of 0.5. At the rear of the cavity, overall coherence levels are much lower for both configurations, consistent with the literature.[7,28] However, the simple rectangular cavity still has a coherent peak above 0.9 at the second mode. This almost perfectly coherent mode again highlights the highly resonant and ordered flow in the rectangular cavity. The baseline cavity, on the other hand, has a peak coherence near 0.5, which occurs for the high frequency fifth mode. These results are consistent with the dominant modes seen in the cross correlations and PSD's.

Similar results were observed at higher Mach numbers. Figs. 11(a) and 11(c) show comparisons between the simple and baseline cavity results at Mach 2.0 and 2.5 at the front of the cavities. As at Mach 1.5, the frequency of the first few modes remains approximately the same as the rectangular cavity while the amplitude of these modes is decreased in the baseline configuration. Once again, then higher modes shift in frequency by about 200 Hz and also increase in magnitude compared to the rectangular cavity. However, the frequency shift is in the opposite direction than was seen at Mach 1.5, a result not predicted by Heller and Bliss for changes with L/D. The time lag in the cross correlations is larger for the baseline cavity at higher Mach numbers, consistent with this observation. At the rear of the cavity, the rectangular geometry again has much higher broadband fluctuation amplitudes. The marked difference in behavior between the two configurations across all Mach numbers is consistent with the shear layer being lifted higher with respect to the aft cavity wall. This weakens the typical feedback mechanisms between the unsteady shear layer and the cavity acoustics that are dominant in the simple cavity and could also explain the change in dominant mode behavior between the two configurations.

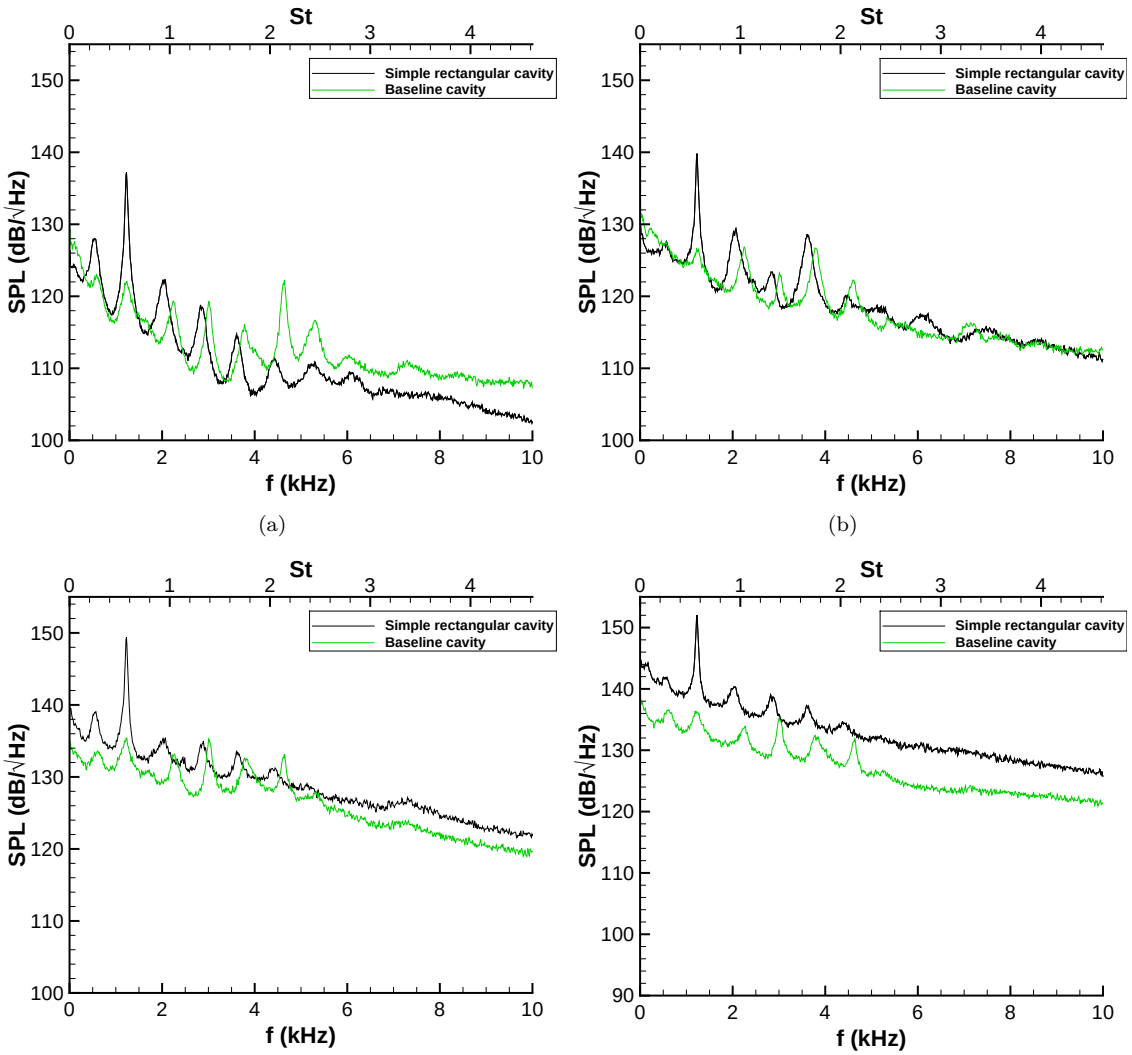

Figure 8. Comparison of simple and baseline cavity power-spectral densities at Mach 1.5 (a) FFP3; (b) C5; (c) RFP3; (d) AWP6.

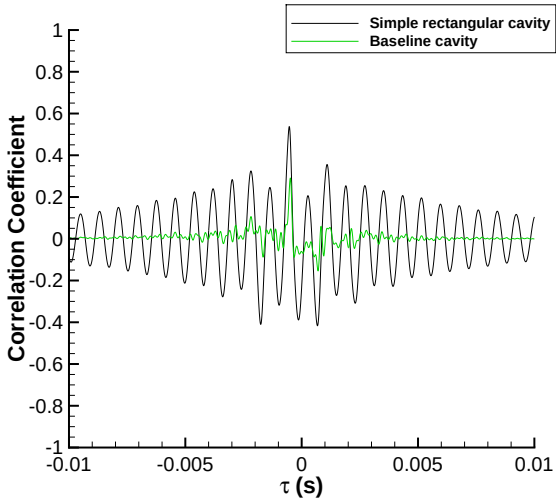

(a)

Figure 9. Comparison of simple and baseline cavity fore-aft cross correlation at Mach 1.5.

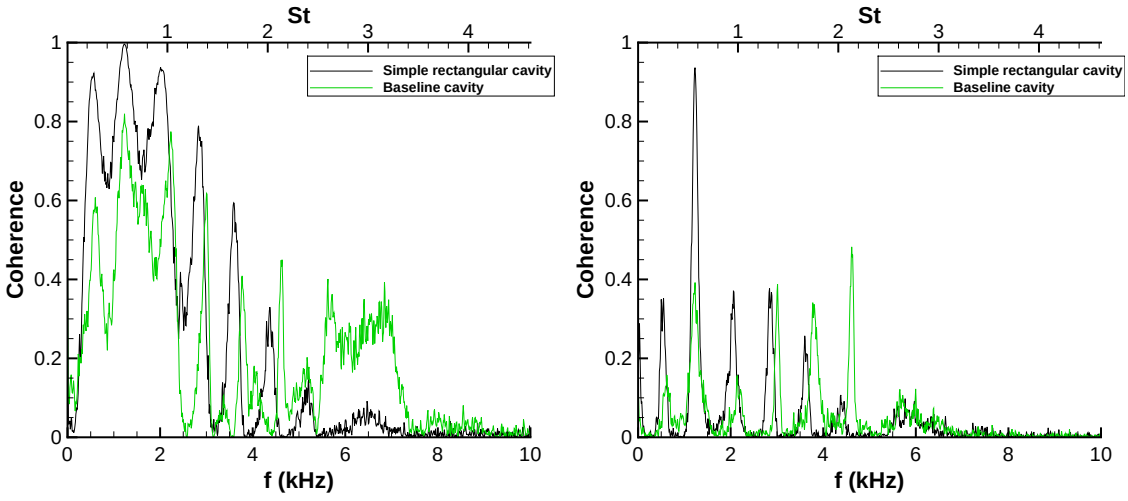

(a) (b)

Figure 10. Comparison of simple and baseline cavity coherences at Mach 1.5 (a) Front (FFP2–FFP4); (b) Rear (RFP2–RFP4).

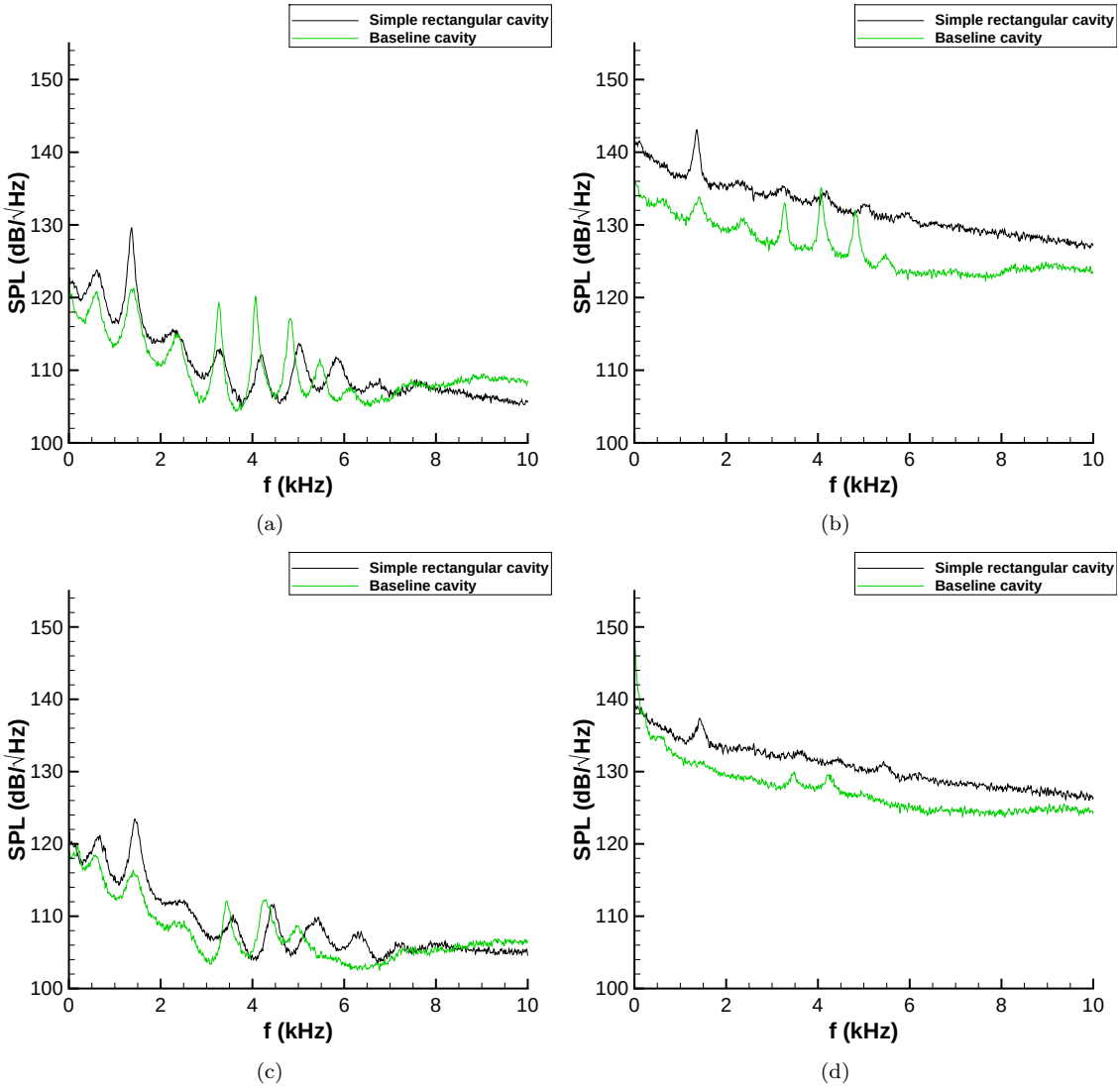

Figure 11. Comparison of power spectral densities in simple and baseline cavities at higher Mach numbers (a) Mach 2, FFP3; (b) Mach 2, AWP6; (c) Mach 2.5, FFP3; (d) Mach 2.5, AWP6.

III.C. Effect of cavity inlet flow

The effect of a nonuniform cavity inlet flow was studied by varying the inlet ramp geometry as compared to the baseline cavity configuration. Both a centered (Fig. 3(b)) and offset scoop (Fig. 3(d)) were tested. A comparison of the PSD's between the different configurations at Mach 1.5 is shown in Fig. 12. Results at other supersonic Mach numbers were qualitatively similar. There are no large differences between the center and offset scoops; they appear similar throughout the cavity in both the level of broadband fluctuations and the mode amplitudes. The frequency of the modes also agrees well with the baseline cavity measurements. As before, modes one and two have similar frequencies as the rectangular cavity (shifted approximately 50 Hz) while the other modes are shifted to higher frequencies by 100–300 Hz. However, the level of broadband fluctuations deviates from the baseline cavity measurements with downstream distance. By the end of the cavity, the broadband fluctuations and mode amplitudes are significantly higher than for the baseline cavity and instead approach the levels of the simple rectangular cavity.

This similarity of the aft wall results to the rectangular cavity measurements likely come from the reduced depth of the cavity along the center of the scoops which brings the shear layer back down towards the aft cavity wall. This would be expected to increase the fluctuations on the rear wall and also enhance the feedback loop feeding the mode amplitudes.[3,15–18] However, even though the broadband fluctuations are higher for both the center and offset scoops, mode two is still significantly reduced in amplitude in comparison with the rectangular cavity. The spanwise nonuniformity introduced by leading edge scoop geometry likely disrupts the shear layer and its uniform impingement on the rear wall which reduces the mode amplitude in comparison to the rectangular cavity.

Cross correlations for these geometries are shown in Fig. 13. The two scoop geometries have intermediate levels of correlation compared to the rectangular and baseline configurations. The correlation also has a periodic behavior, but at a lower frequency near 600 Hz corresponding to the first Rossiter mode. The coherence of the pressure signals also confirms that the first mode has the highest coherence for the two scoop geometries, near 0.5, significantly higher than for the baseline cavity (Fig. 14). The second mode also has coherence levels near 0.5, but this is much lower than the coherence level above 0.9 seen for the rectangular cavity. These results are consistent with the corresponding PSD's which show that the first mode is dominant for these configurations at the rear wall, and of equal amplitude to the second mode at other locations in the cavity.

III.D. Effect of cavity leading edge configuration: asymmetric tooth

To simulate a typical flight geometry, an asymmetric tooth was added to the leading edge of the complex geometry in conjunction with the different ramp configurations (Figs. 3(c) and 3(e)). This tooth affects the measured pressure spectra. Fig. 15 shows typical results at Mach 1.5; other Mach numbers showed similar trends and are not shown. At the upstream end of the cavity under the tooth, the amplitude of modes two and three are enhanced while higher frequencies appear to be suppressed. This enhancement is likely because the tooth creates an overhang at the front of the cavity that constricts the flow and leads to additional resonances in that location. However further downstream, the tooth tends to reduce the amplitude of both the modes and broadband frequencies. This reduction could result from the tooth disrupting the spanwise coherence of the shear layer which could reduce cavity fluctuations.[16,17] The streamwise vorticity generated by the tooth also takes some distance to grow, so it would be expected to have less effect on the shear layer upstream and more effect downstream.

Cross correlations between different locations in the cavity (Fig. 16) show that the tooth does modify the correlation levels between the fore and aft of the cavity. Lower frequencies are more correlated, while others appear to be reduced. The coherence in the cavity (Fig. 17) shows that lower modes have higher levels of coherence with the tooth at the front of the cavity, while the coherence of higher modes is lower, especially at the rear of the cavity. These observations are consistent with the PSD's that show dominance of the lower modes at the front of the cavity, but lower amplitudes further downstream. Overall, the presence of the tooth reduces the pressure fluctuations over the majority of the cavity.

The offset tooth has a similar effect on the flow as the center tooth; it enhances some modes near the front of the cavity but reduces the mode amplitudes further downstream. However, the magnitude of the mode enhancement and reduction at different parts of the cavity is slightly smaller overall. The similarity of the offset and center tooth results is consistent with the small differences observed between the center and offset scoop geometries as discussed in Sec. III.C.

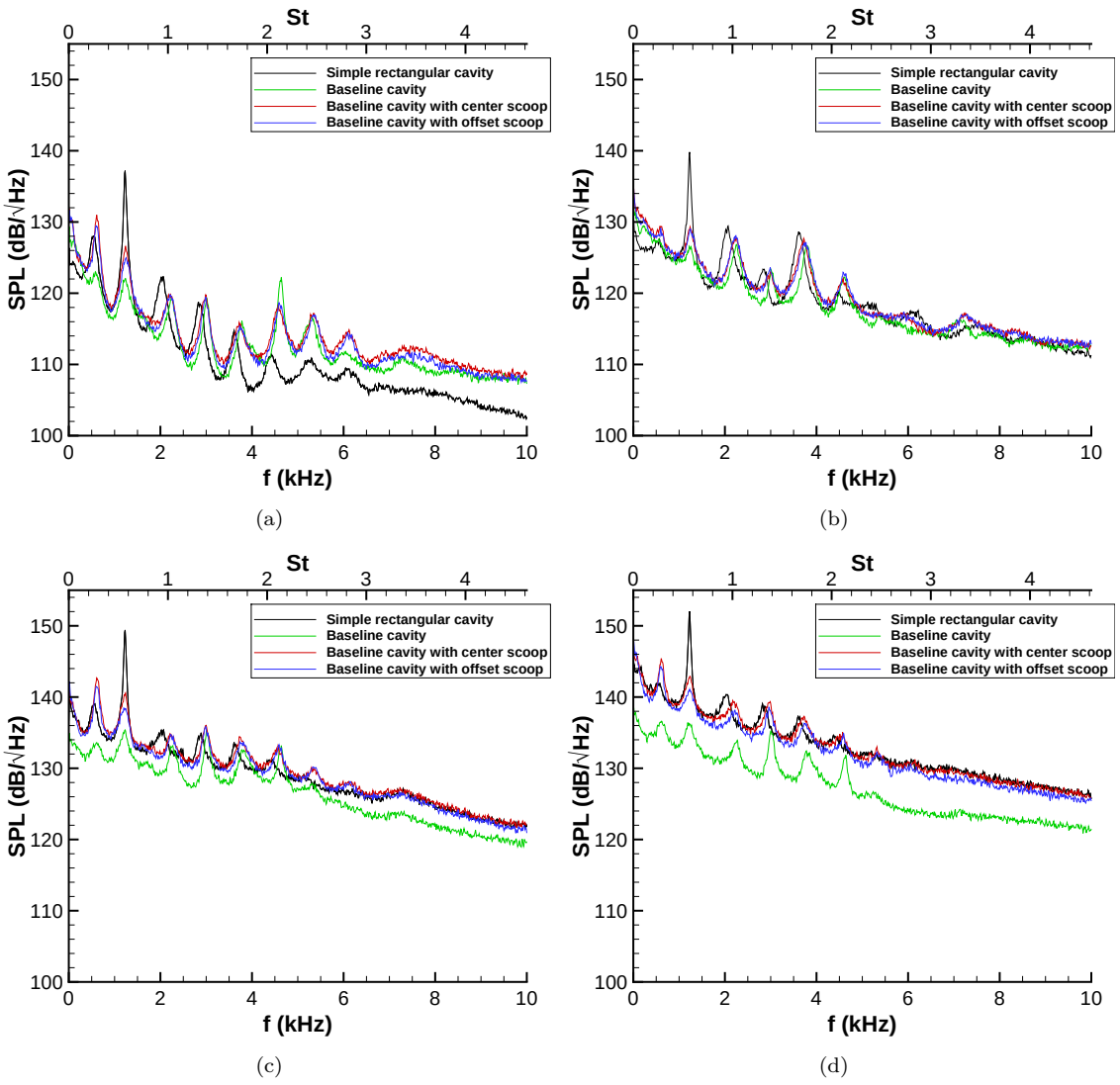

Figure 12. Effect of cavity inlet flow at Mach 1.5 (a) FFP3; (b) C5; (c) RFP3; (d) AWP6.

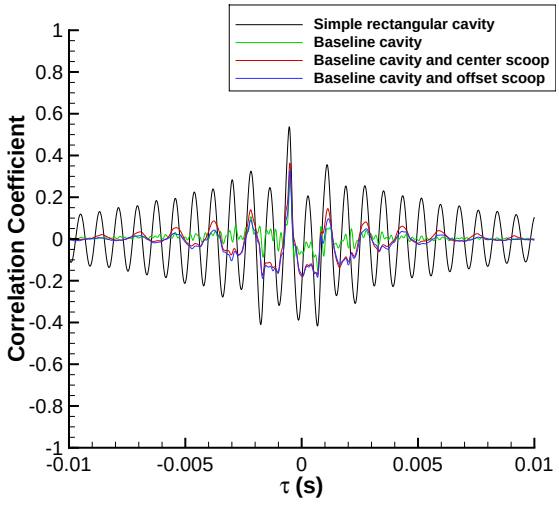

Figure 13. Effect of cavity inlet flow at Mach 1.5 on fore-aft cross correlation.

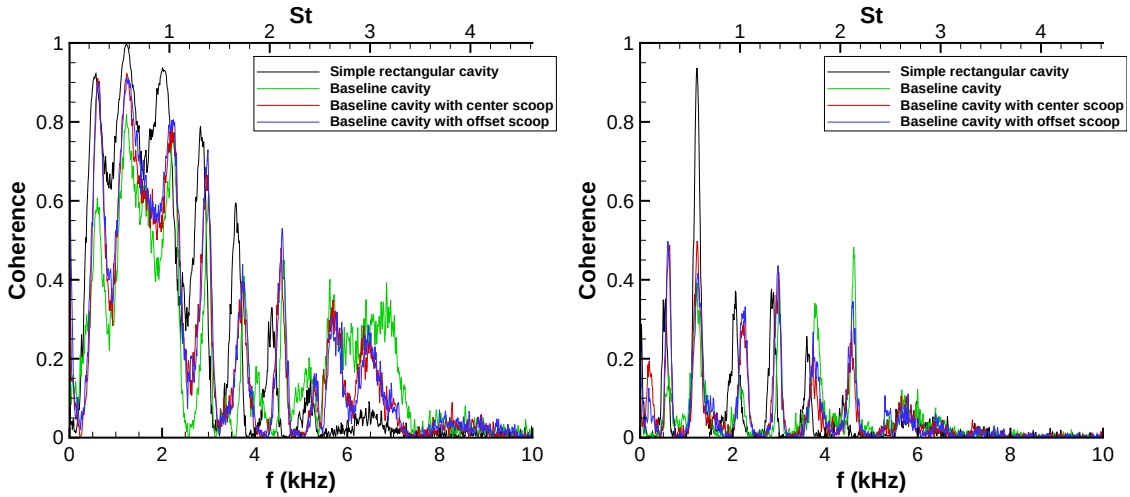

Figure 14. Effect of cavity inlet flow at Mach 1.5 on coherence (a) Fore coherence (FFP2-FFP4); (b) Rear coherence (RFP2-RFP4).

III.E. Effect of changing L/W: side insert

Varying internal geometry can also affect the cavity pressure fluctuations. Fig. 18 shows PSD's of the pressure fluctuations in the complex geometry, with and without the side insert at Mach 1.5. Again, qualitative similarity was seen at other Mach numbers. The insert has a significant effect on the cavity flow, primarily in the upstream end of the cavity and in front of the insert. Most of the Rossiter modes are enhanced, with the exception of the third mode. There is no frequency shift of the modes which is expected since the L/D of most of the cavity does not change in this configuration. The side insert also results in much higher broadband fluctuations than are observed without the side insert. This influence decreases somewhat along the centerline and further downstream, though the higher frequencies still remain elevated even on the aft cavity wall. Other configurations with the side insert showed similar enhancements of the higher frequency modes and broadband fluctuations, especially in front of the side insert and at the upstream end of the cavity.

Cross correlations of pressure fluctuations within the cavity show higher and more periodic correlation levels with the presence of the side insert (Fig. 19). The primary frequency of this periodicity is near 1.3 kHz, consistent with the highest amplitude second mode seen in the PSD's with the presence of the side insert. The coherence in the cavity (Fig. 20) also shows that this second mode has the highest coherence level of all the cavity modes with the side insert. This mode remains highly coherent even at the rear wall, leading to more organized and periodic fluctuations within the cavity. This enhanced resonance may result from the shorter cavity on one side of the configuration. The reduced length means that the shear layer would impinge slightly lower with respect to the front of the side insert in comparison with the aft cavity wall. This may lead to more cavity resonance and the higher second mode amplitude observed in the PSD's.

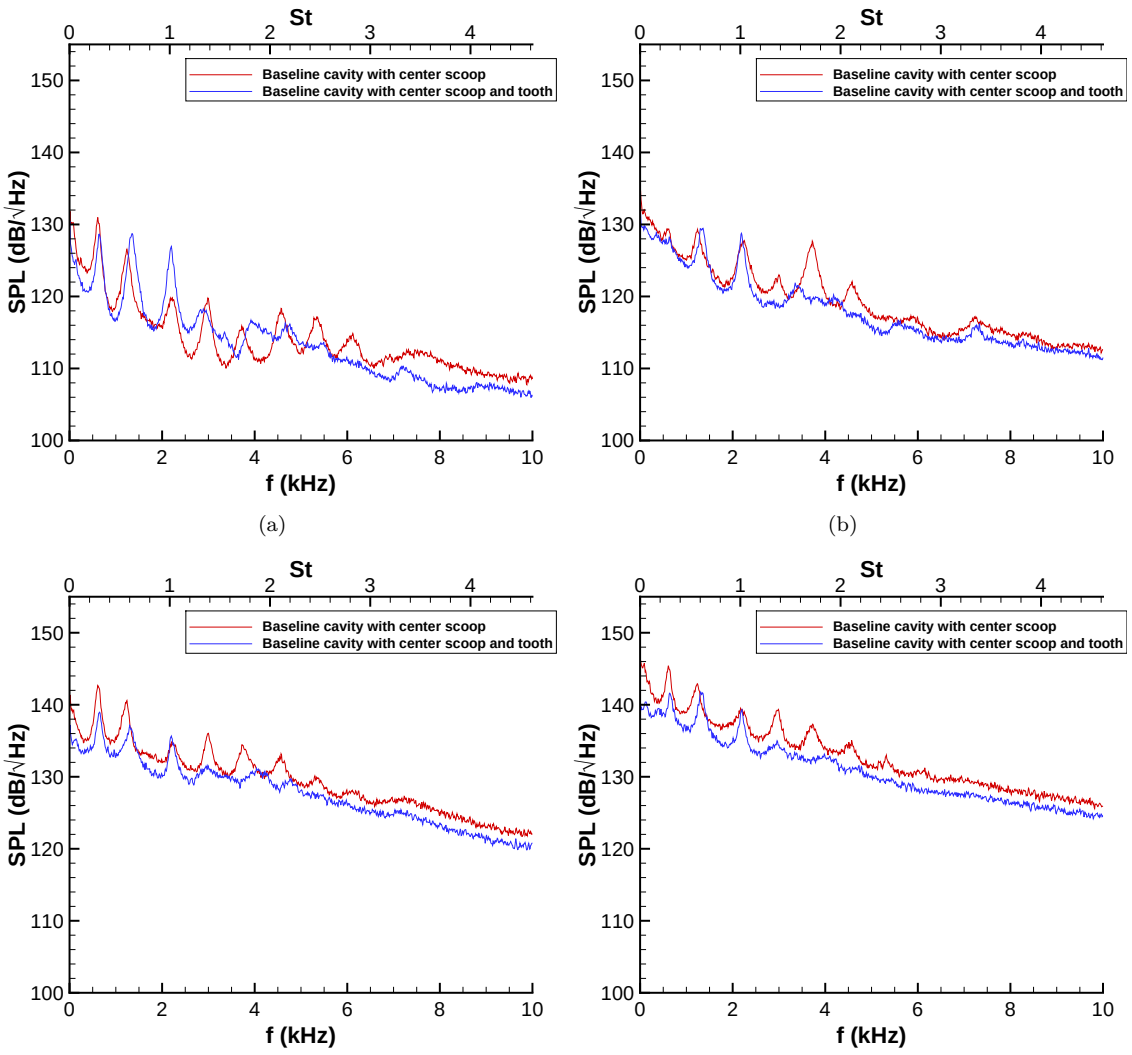

Figure 15. Effect of leading edge tooth at Mach 1.5 on power-spectral densities (a) FFP3; (b) C5; (c) RFP3; (i) AWP6.

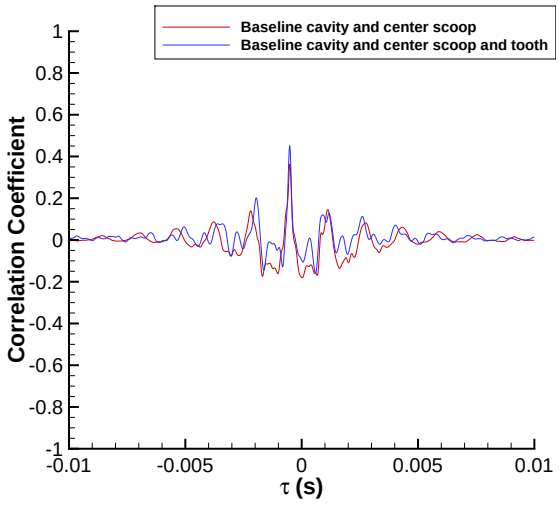

Figure 16. Effect of leading edge tooth at Mach 1.5 on fore-aft cross correlation.

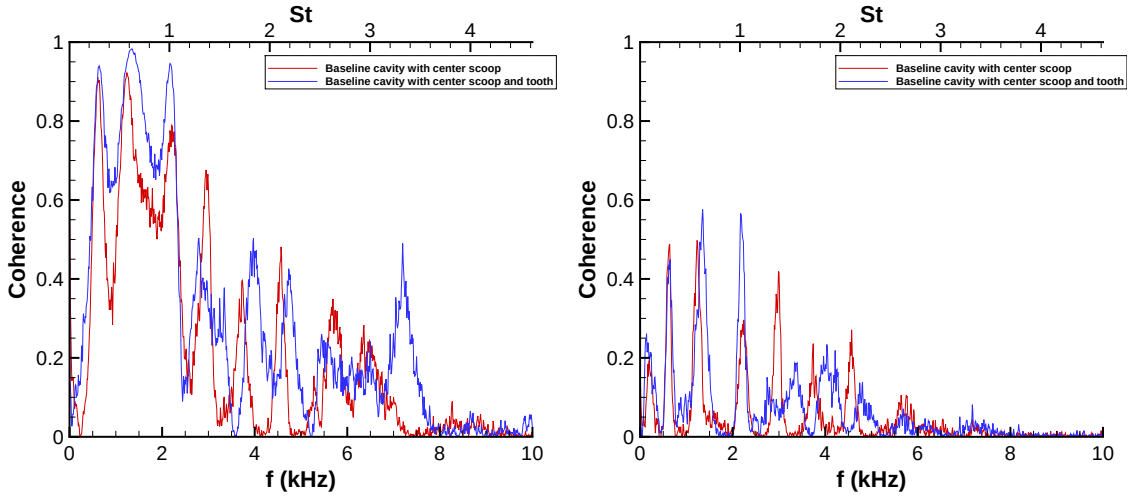

Figure 17. Effect of leading edge tooth at Mach 1.5 on coherence (a) Front (FFP2–FFP4); (b) Rear (RFP2–RFP4).

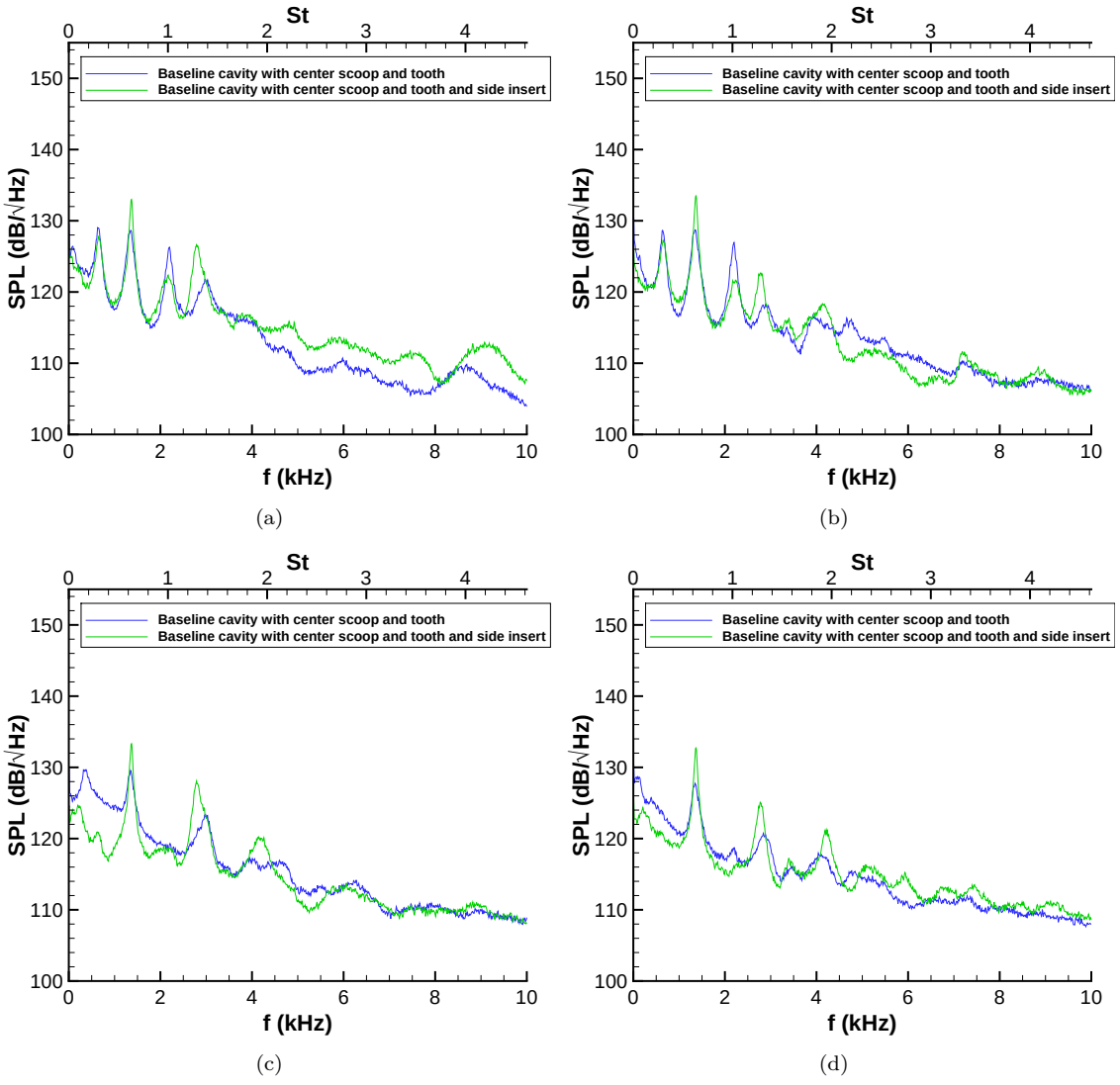

Figure 18. Effect of side insert at Mach 1.5 on power-spectral densities (a) FFP5; (b) FFP3; (c) R4; (d) C4.

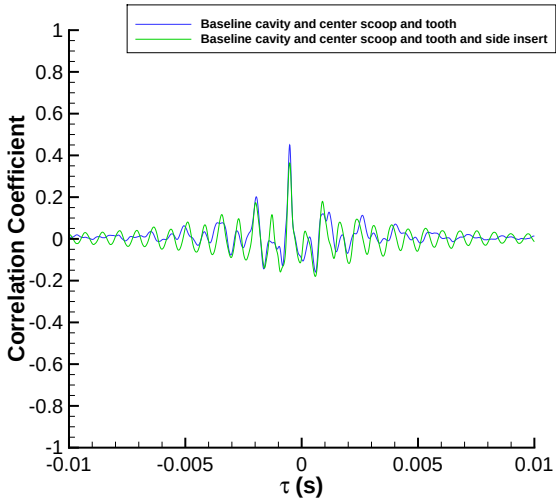

(a)

Figure 19. Effect of side insert at Mach 1.5 on fore-aft cross correlation.

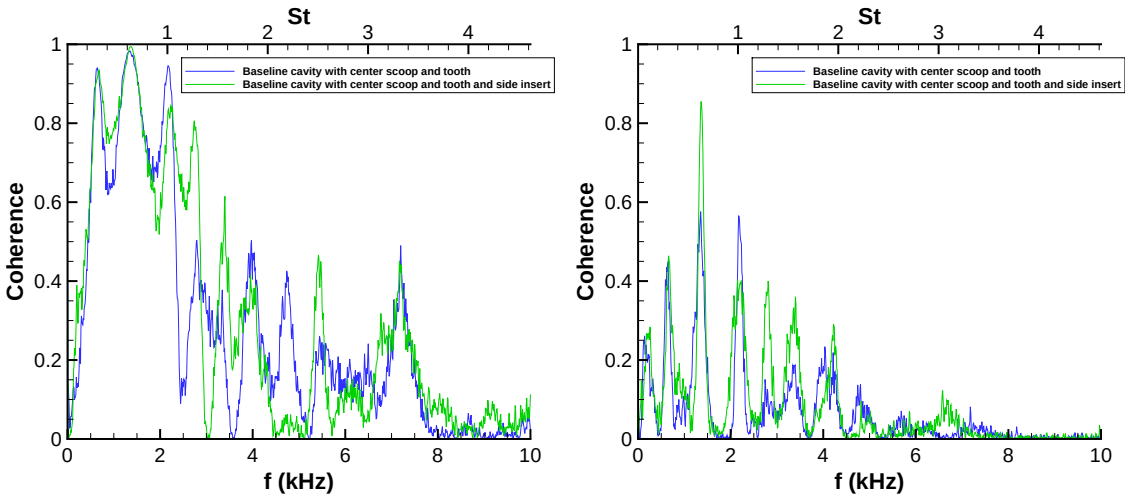

(a) (b)

Figure 20. Effect of side insert at Mach 1.5 on coherence (a) Front (FFP2–FFP4); (b) Rear (RFP2–RFP4).

IV. Concluding Remarks and Future Work

A complex cavity has been designed to allow representative features of a weapons bay to be incorporated into a basic rectangular cavity. This allows the effect of each of these features on the cavity flow to be isolated and studied. Tests were conducted in the Sandia Trisonic Wind Tunnel at supersonic Mach numbers of 1.5, 2.0, and 2.5.

Measurements with a simple rectangular cavity were consistent with the literature. The pressure fluctuations showed resonant peaks at frequencies predicted by theory. The second cavity mode dominated the pressure spectra. High levels of cross correlations and coherence were also observed for this mode, indicating organized and periodic pressure fluctuations in the cavity.

Complex features were then added to the rectangular cavity to modify both the inlet and internal geometry. Some features were found to enhance the pressure fluctuations, primarily any configurations that constricted the flow. This occurred underneath a leading edge tooth that created an overhang at the front of the cavity, and also in front of a side insert that was placed at the aft end of the cavity to simulate internal cavity variations. The cross correlation and coherence levels of the enhanced modes typically increased, indicating more organized and periodic fluctuations associated with those enhanced modes.

Other geometric changes could suppress the cavity resonances if they interfered with the unsteady shear layer over the cavity. A leading edge ramp that lifted the shear layer higher with respect to the aft cavity wall had the largest effect. Both the mode amplitudes and broadband fluctuations at the aft end of the cavity were significantly reduced. This also decreased the cross correlation and coherence levels within the cavity. Other configurations that added additional spanwise non-uniformity to the incoming flow such as a scooped inlet geometry or the presence of a leading edge tooth appeared to interfere with the shear layer and led to a reduction in mode amplitudes and broadband fluctuations, especially at the rear wall of the cavity.

The physical mechanisms that led to these changes still need to be explored further. Additional experiments will be conducted simultaneous with PIV to better understand how the flowfield couples with the complex cavity features. This work is also being conducted in the subsonic regime where choking difficulties are reduced, which will allow the effect of the doors to be studied. Subsonic testing has been focused on interference from wind tunnel duct resonance modes before a sweep of complex geometry configurations is conducted.[29] Once the empty cavity configurations have been tested, a store will also be introduced to study the fluid-structure interactions that occur in the complex geometry. Ongoing work also continues to compute these complex flows, for comparison to the experimental database.

Acknowledgments

The authors thank Srinivasan Arunajatesan and Matthew Barone for helpful discussions on cavity dynamics. Tom Grasser designed and oversaw construction of the complex geometry hardware.

References

[1]Rockwell, D. and Naudascher, E., "Review-Self-Sustaining Oscillations of Flow Past Cavities," *Journal of Fluids Engineering*, Vol. 100, No. 2, 1978, pp. 152–165.

[2]Rowley, C. W. and Williams, D. R., "Dynamics and Control of High-Reynolds-Number Flow over Open Cavities," *Annual Review of Fluid Mechanics*, Vol. 38, 2006, pp. 251–276.

[3]Rossiter, J. E., "Wind-Tunnel Experiments on the Flow over Rectangular Cavities at Subsonic and Transonic Speeds," Reports & Memoranda 3438, Aeronautical Research Council, October 1964.

[4]Stallings, R. L. and Wilcox, F. J., "Experimental Cavity Pressure Distributions at Supersonic Speeds," NASA Technical Paper 2683, June 1987.

[5]Dix, R. E. and Bauer, R. C., "Experimental and Theoretical Study of Cavity Acoustics," Tech. Rep. AEDC-TR-99-4, Arnold Engineering Development Center, May 2000.

[6]Heller, H. H. and Bliss, D. B., "The Physical Mechanism for Flow-Induced Pressure Fluctuations in Cavities and Concepts for their Suppression," AIAA Paper 75-491, March 1975.

[7]Wagner, J. L., Casper, K. M., Beresh, S. J., Hunter, P. S., Spillers, R. W., Henfling, J. F., and Mayes, R. L., "Experimental Investigation of Fluid-Structure Interactions in Compressible Cavity Flows," AIAA Paper 2013-3172, June 2013.

[8]Wagner, J. L., Beresh, S. J., Casper, K. M., Henfling, J. F., Spillers, R. W., Hunter, P. S., Blecke, J. C., and Mayes, R. L., "Simultaneous Vibration and Acoustic Measurements of a Store in Compressible Open Cavity Flow," AIAA Paper 2013-0228, January 2013.

[9]Beresh, S. J., Wagner, J. L., and Pruett, B. O. M., "Supersonic Flow over a Finite-Width Rectangular Cavity," AIAA Paper 2013-0389, January 2013, also submitted to AIAA Journal.

[10]Kannepalli, C., Chartrand, C., Birkbeck, R., Sinha, N., and Murray, N., "Computational Modeling of Geometrically Complex Weapons Bays," AIAA Paper 2011-2774, June 2011.

[11]Plentovich, E., Chu, J., and Tracy, M. B., "Effects of Yaw Angle and Reynolds Number on Rectangular-Box Cavities at Subsonic and Transonic Speeds," Tech. Rep. NASA TP-3099, 1991.

[12]Disimile, P. J., Toy, N., and Savory, E., "Pressure Oscillations in a Subsonic Cavity at Yaw," *AIAA Journal*, Vol. 36, No. 7, July 1998, pp. 1141–1148.

[13]Lee, B. H. K., Orchard, D. M., and Tang, F. C., "Flow Past a Yawed Rectangular Cavity in Transonic and Low Supersonic Flows," *Journal of Aircraft*, Vol. 46, No. 5, September – October 2009, pp. 1577–1583.

[14]Tracy, M. B., Plentovich, E. B., Hemsch, M. J., and Wilcox, F. J., "Effect of Sweep on Cavity Flow Fields at Subsonic and Transonic Speeds," Tech. Rep. NASA TM 2012-217577, NASA Langley Research Center, May 2012.

[15]Cattafesta, L., Williams, D. R., Rowley, C. W., and Alvi, F., "Review of Active Control of Flow-Induced Cavity Resonance," AIAA Paper 2003-3567, June 2003.

[16]Ukeiley, L., Sheehan, M., Coiffet, F., Alvi, F., Arunajatesan, S., and Jansen, B. J., "Control of Pressure Loads in Geometrically Complex Cavities," *Journal of Aircraft*, Vol. 45, No. 3, May–June 2008, pp. 1014–1024.

[17]Arunajatesan, S., Kannepalli, C., Sinha, N., Sheehan, M., Alvi, F., Shumway, G., and Ukeiley, L., "Suppression of Cavity Loads Using Leading-Edge Blowing," *AIAA Journal*, Vol. 47, No. 5, May 2009, pp. 1132–1144.

[18]Dudley, J. G. and Ukeiley, L., "Suppression of Fluctuating Surface Pressures in a Supersonic Cavity Flow," AIAA Paper 2010-4974, June 2010.

[19]Shaw, L., Clark, R., and Talmadge, D., "F-111 Generic Weapons Bay Acoustic Environment," AIAA Paper 87-0168, January 1987.

[20]Murray, N. E. and Jansen, B. J., "Effect of Door Configuration on Cavity Flow Modulation Process," *AIAA Journal*, Vol. 50, No. 12, December 2012, pp. 2932–2937.

[21]Panickar, M. B., Murray, N. E., Jansen, B. J., Joachim, M. P., Birkbeck, R., Kannepalli, C., and Sinha, N., "Reduction of Noise Generated by a Half-Open Weapons Bay," *Journal of Aircraft*, Vol. 50, No. 3, May–June 2013, pp. 716–724.

[22]Stallings, R. L., Plentovich, E., Tracy, M. B., and Hemsch, M. J., "Measurements of Store Forces and Moments and Cavity Pressure for a Generic Store In and Near a Box Cavity at Subsonic and Transonic Speeds," Tech. Rep. NASA TM-4611, May 1995.

[23]Lee, B. H. K., "Effect of Cavity Store on Internal Weapons Bay Floor Pressure Distributions," *Journal of Aircraft*, Vol. 47, No. 2, March–April 2010, pp. 732–735.

[24]Bartel, H. W. and McAvoy, J. M., "Cavity Oscillation in Cruise Missile Carrier Aircraft," Tech. Rep. AFWAL-TR-81-3036, Air Force Wright Aeronautical Laboratories, June 1981.

[25]Kegerise, M. A., *An Experimental Investigation of Flow-Induced Cavity Oscillations*, Ph.D. Thesis, Syracuse University, August 1999.

[26]Tracy, M. B. and Plentovich, E. B., "Cavity Unsteady-Pressure Measurements and Subsonic and Transonic Speeds," NASA Technical Paper 3669, December 1997.

[27]Murray, N., Sällström, E., and Ukeiley, L., "Properties of Subsonic Open Cavity Flow Fields," *Physics of Fluids*, Vol. 29, 2009, pp. 1–16, 095103.

[28]Zhuang, N., Alvi, F., Alkislar, M. B., and Shih, C., "Supersonic Cavity Flows and Their Control," *AIAA Journal*, Vol. 44, No. 9, September 2006, pp. 2118–2128.

[29]Wagner, J. L., Casper, K. M., Beresh, S. J., Henfling, J. F., Spillers, R. W., and Pruett, B. O. M., "Mitigation of Wind Tunnel Modes in Subsonic Cavity Flows," AIAA Paper, to appear, June 2014.